

Challenges of design and fabrication technology of plasmonic components for Photonic Integrated Circuits (Invited)

Vadym Zayets*^a, Iryna Serdeha^b, Valerii Grygoruk^b

^aPlatform Photonics Research Center (PPRC), National Institute of Advanced Industrial Science and Technology (AIST), Tsukuba, Japan 305-8568; ^b Quantum Radio-Physics Department, Taras Shevchenko National University of Kyiv, Kyiv, Ukraine 01601

ABSTRACT

The two unique features of the plasmonic devices are their small size of about 10-100 μm and their technological compatibility with the Photonic Integrated Circuits (PIC). These features make them attractive as components for a denser and smaller PIC. We have developed and experimentally demonstrated a fabrication technology, which allows a substantial decrease of the plasmonic propagation loss for both a “plasmon- friendly” metal like Au, Cu or Al and “plasmon- unfriendly” metal like Co, Fe or Cr. In each case the propagation can be reduced below 1 dB per plasmonic device. The developed technologies are based on the optimization of the optical confinement for a surface plasmon. A moderate coupling loss of 4 dB per facet between plasmonic and Si waveguide is still a problem for the in-series integration, but it can be resolved by a usage of in-parallel integration of the plasmonic and Si waveguides. A low propagation loss of 0.7 dB/ μm was achieved for a surface plasmon in a Co/TiO₂/SiO₂ plasmonic structure on a Si substrate. The low insertion loss of 0.9 dB and 2 dB at $\lambda=1550$ nm was demonstrated for the parallel integration of a Co/TiO₂/SiO₂ plasmonic waveguide and a Si waveguide for gap of 600 nm and of 250 nm between waveguides, respectively.

Keywords: Plasmonic, optical isolator, dense optical integration

1. PLASMONIC AND DENSE OPTICAL INTEGRATION

Surface plasmon is a quasiparticle of collective electron oscillations coupled to electromagnetic waves at the interface between materials having positive and negative permittivity, typically a dielectric and a metal¹⁻³. A uniqueness of a surface plasmon is its topological nature meaning that optical confinement of the plasmon as well as all plasmon's properties are defined by optical properties of a surface, but not of the bulk as in the case of a conventional optical waveguide. Even a small change of optical properties in close proximity of the interface substantially modifies plasmon's propagation constants. It makes it possible to modulate light within propagation distance of only a few wavelengths and, therefore, to fabricated plasmonic devices of a small size for a dense optical integration.

The monolithic integration of the plasmonic devices with Si nanowire waveguides is the most beneficial. Ability of a dense integration is the most attractive feature of both the Si nanowire waveguides and the plasmonic waveguides. Similar to electronic integrated devices, a dense-integrated optical circuit may benefit of a lower cost and better functionality. However, there is a problem for a dense integration of optical components and the problem is the size of the optical components. In the case of an electronic circuit, the size of MOSFET transistors is very small and billions of transistors can be integrated into one electrical circuit. Because of the dense integration, the integrated electronic devices have a complex functionality at a low cost. In contrast, the size of optical components is not as small. The typical length of optical components is about a millimeter⁴ and only a few optical components can be integrated into one chip. The length of optical components is limited by the wavelength of light and a small possible change of the refractive index. In a practical optical device, the largest change of the refractive index does not exceed a few percent and light needs to propagate thousands of wavelengths in order to accumulate such a small change into a sizable effect. It is possible to substantially reduce the size of an optical component, when an optical waveguide having a strong optical confinement such as a Si nanowire waveguide is used. Since the width of the Si waveguide is narrow (~ 420 nm), the waveguide can be bent back and forward within a small area and a large effect can be accumulated in a small- foot-print device. The optical confinement in a Si waveguide is strong, because of a high refractive index contrast between Si and SiO₂ and,

*v.zayets@gmail.com; phone +81-298-61-5426; web: <https://staff.aist.go.jp/v.zayets/>

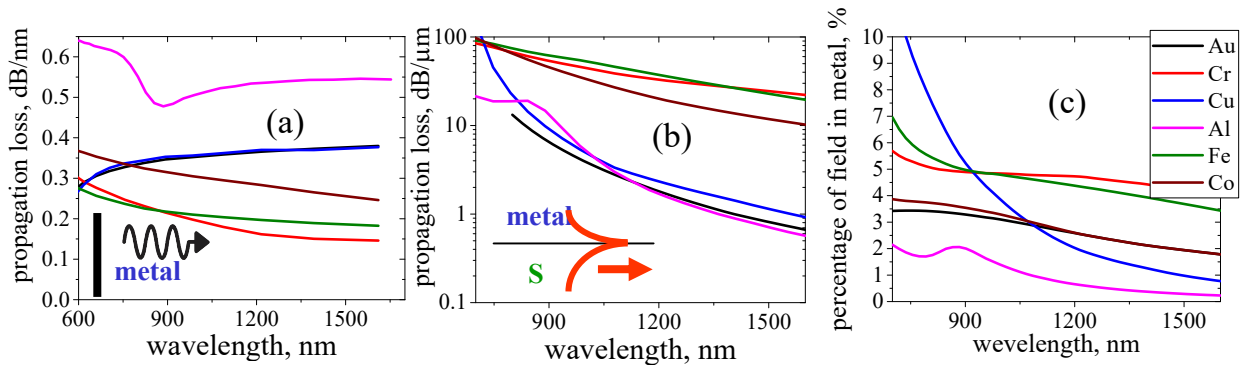


Figure 1. (a) Propagation loss of light propagating in the bulk of a metal. (b) Propagation loss of a surface plasmon propagating at a metal/ Si interface. Because of a large difference of loss, a different unit is used for graphs (a) and (b). (c) Percentage of optical field in metal for a surface plasmon propagating at a metal/ Si interface. Data is calculated from integration of distribution of the optical field across interface.

therefore, they can sharply bend with a bending radius as small⁴ as 1 μm. A change of propagation constants of a surface plasmon can be substantial even within a short propagation length of about 10 μm and, therefore, the accumulation of the effect is not required for a plasmonic device. It means that plasmonic devices are inherently of a very small size³.

2. EFFECTIVE PLASMON CONFINEMENT AS A SOLUTION FOR REDUCTION OF PLASMONIC LOSS

A metal absorbs light and, therefore, the propagation loss is unavoidable for a surface plasmon. However, when design and fabrication technology of a plasmonic device are optimized, the loss due to the light absorption by the metal is negligibly small^{3,5-8} and does not degrade the plasmonic device. Still the optical loss is the key issue for any plasmonic device and should be carefully addressed. Below, the technological methods⁶⁻⁹ of a fabrication of a loss- loss plasmonic waveguides are explained.

There is a misconception that there are “plasmon- friendly” metals like Au, Al, Cu, because their absorption of light is weaker and only they should be used for a plasmonic device^{1,10}, and there are “plasmon- unfriendly” metals like Co, Fe, Cr, because their absorption of light is much stronger and these metals should not be used in a plasmonic device. Figure 1(a) shows the calculated propagation loss of light propagating in the bulk of a metal using data of Ref.[¹¹]. In fact, the absorption loss in the “plasmon- friendly” metals is larger than in the “plasmon- unfriendly” metals. The smallest absorption is in the “plasmon- unfriendly” chromium and the largest absorption is in the “plasmon- friendly” aluminum.

Figure 1(b) shows the calculated propagation loss of a surface plasmon propagating along a metal/ Si interface. Indeed, the Au, Al, Cu have a substantially smaller plasmon propagation loss of about 1 dB/μm at λ=1550 nm. E.g., in the case of a 5-μm- long plasmonic device made of these metals, the insertion loss due to metal absorption is about 5 dB. It is still large but could be acceptable for some applications. In contrast, plasmonic propagation loss is huge (~20 dB/μm) in the plasmonic structure containing Fe, Co and Cr. Even in a 1-mm-long plasmonic device, nearly all light is absorbed and, therefore, such plasmonic structure cannot be used in PIC. What is the reason why the plasmonic loss is larger for a metal having a small intrinsic absorption coefficient of light? Figure 2(a) shows the relative amount of optical field in metal calculated for the surface plasmon of Fig.1(b). In the case of iron and chromium, there is a large amount of optical field of about 5 % inside of metal. In contrast, the amount is less 0.5 % in the case of aluminum. That is the reason why the plasmonic absorption is substantially smaller in the aluminum in comparison to the iron and chromium despite the bulk absorption in Al is substantially larger (see Fig. 1a).

It is not only the bulk absorption by a metal, but also the refractive index of the metal that determines the absorption of a surface plasmon. The metal refractive index affects both the skin depth in a metal and the penetration depth of the optical field into dielectric. At λ=1550 nm the calculated skin depth in a metal is 15, 40 and 50 nm and the calculation penetration depth of the optical field into the dielectric is 300, 151 and 187 nm for Al/Si, Fe/Si and Cr/Si interfaces,

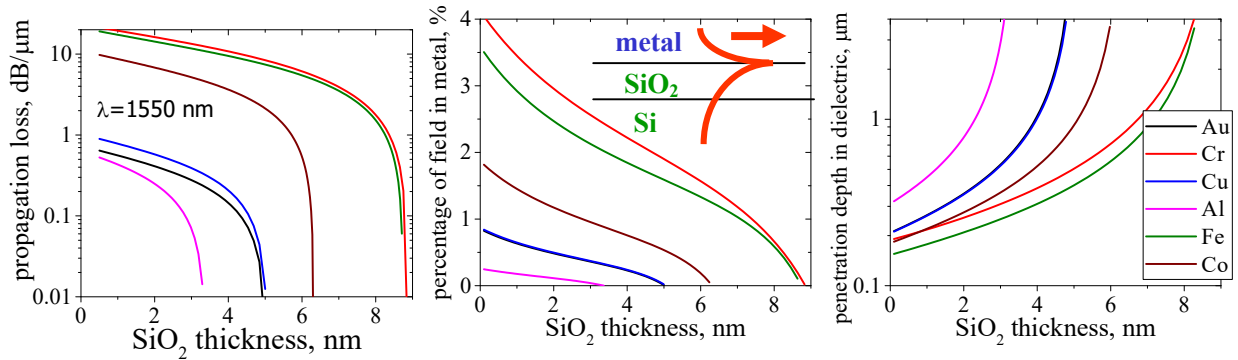


Figure 2. (a) Propagation loss of a surface plasmon in metal/ SiO₂/ Si structure as a function of SiO₂ thickness. For each metal there is an optimum SiO₂ thickness for which the loss is equally small for each metal.

correspondingly. Both the smaller skin depth in metal and the larger penetration depth into Si are reasons why the amount of light penetrating in Al is smaller than that penetrating in Fe and Cr.

The amount of light penetrating into the metal can be engineered and reduced in a more complex plasmonic structure, which contains more dielectric layers^{5,10,12,13}. As a result, a low- absorption plasmonic structure can be designed for both the “plasmon- friendly” and “plasmon- unfriendly” metals. For example, we have fabricated and studied a Co-based and Fe- based magneto-optical plasmonic structure (See Section 3) for over 10 years and the absorption loss has never been an issue as soon as the described technology was followed.

It is difficult to change substantially the skin depth in a metal. In contrast, the penetration depth into dielectric depends significantly on the type and the structure of the dielectric and, therefore, can be engineered. As a result, the relative amount of optical field in metal can be reduced, which leads to the reduction of propagation loss of a surface plasmon. An insertion of a thin dielectric layer of a different refractive index at the boundary between the metal and the dielectric is effective for the reduction. Figure 2(a) shows the calculated propagation loss in a metal/SiO₂/Si plasmonic structure. For both the “plasmon- friendly” and “plasmon- unfriendly” metals, the propagation loss can be reduced down to 0.01 dB/μm at an optimum SiO₂ thickness. The optimum SiO₂ thickness is different for each metal. It means that for a 10-mm-long plasmonic device the absorption loss is only 0.1 dB, which is negligible in comparison to the unavoidable coupling loss (See below). The insertion of a thin SiO₂ layer reduces the amount of plasmon optical field penetrated into the metal. It is the reason for the reduction of the propagation loss. Figure 2(b) shows the percentage of light penetrating into the metal as a function of the SiO₂ thickness. At the optimum thickness, there is nearly no light in the metal.

Even though theoretically it is possible to reduce the plasmonic propagation loss to an infinitely small number, there are technological limitations, which limit the possible reduction. The first limitation is the fabrication precision and roughness of a thin inserted dielectric layer. As can be seen from Fig.2(a), in order to have a similar propagation loss a plasmonic structure containing Cr, Fe, Co requires a better fabrication precision for the SiO₂ thickness than a structure

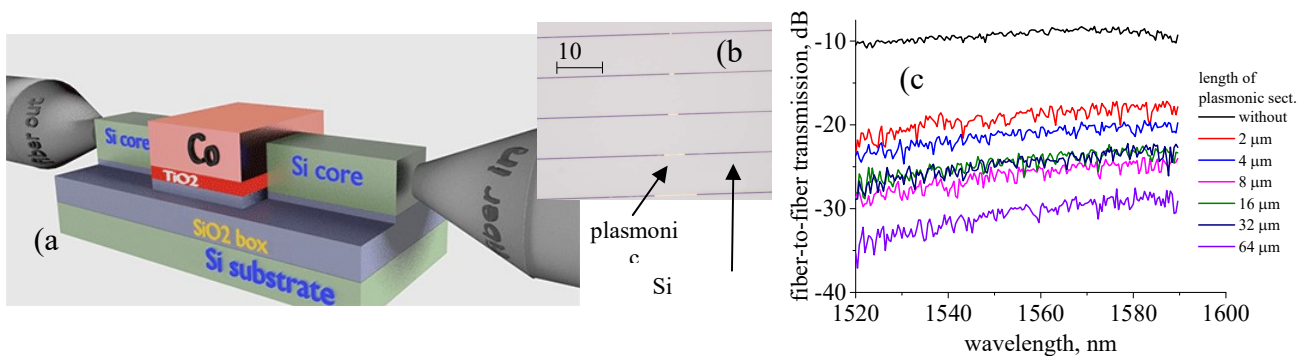


Figure 3 (a) Measurement setup for evaluation of a propagation loss and coupling a Co/TiO₂/SiO₂ plasmonic waveguide integrated with a Si nanowire waveguide; (b) Top view from an optical microscope of Si nanowire waveguide integrated with plasmonic waveguides; (c) Fiber-to-fiber transmission⁷ as function of wavelength for different lengths of Co/TiO₂/SiO₂ plasmonic waveguide integrated with Si nanowire waveguide. Black line shows the case of waveguide without plasmonic part. The bridge type of the in-plane confinement (See Fig.4) was used.

containing Au, Al, Cu. Another technological limitation is the penetration depth of the optical field into the dielectric. It should not exceed 10 μm . Otherwise, the plasmonic properties may become dependent on inhomogeneities and imperfections of the substrate. Figure 2(c) shows the calculated the penetration depth of the optical field into the dielectric as a function of the SiO_2 thickness. For all calculated cases, this condition limits possible reduction at ~ 0.01 $\text{dB}/\mu\text{m}$.

Figure 3a shows the measurement setup for evaluation of a propagation loss and coupling efficiency for a $\text{Co}/\text{TiO}_2/\text{SiO}_2$ plasmonic waveguide integrated with a Si nanowire waveguide. Light is coupled from the input fiber to the Si nanowire waveguide (green) and next into the plasmonic waveguide. Passing through the plasmonic waveguide, light is coupled again into the Si nanowire waveguide and finally into the output fiber. The fabricated device consists of a Si nanowire waveguide, a part of which (about 2-16 μm) is etched out, and Co is deposited in the gap. The ferromagnetic metal is not transparent and the direct light propagation from the input Si waveguide to the output Si waveguide is blocked by the Co. However, a surface plasmon is excited at the $\text{Co}/\text{TiO}_2/\text{SiO}_2$ interface and it makes light to reach the output fiber. Figure 3(b) shows a top view of a $\text{Co}/\text{TiO}_2/\text{SiO}_2$ plasmonic waveguide of different lengths integrated with a Si nanowire waveguide. Figure 3(c) shows the measured fiber-to-fiber transmission as function of wavelength for different lengths of the $\text{Co}/\text{TiO}_2/\text{SiO}_2$ plasmonic waveguide integrated with a Si nanowire waveguide. The transmission loss increases with the length of the plasmonic section. From a measurement of this dependence the propagation loss of a surface plasmon is evaluated¹⁴⁻¹⁶ to be 0.7 $\text{dB}/\mu\text{m}$. The loss extrapolated to the zero length of plasmonic section gives the coupling loss between plasmonic and Si nanowire waveguides of 4 dB per a facet. The fiber-to- Si-waveguide loss is evaluated¹⁴⁻¹⁶ to be 4.5 dB per facet from a measurement of a Si waveguide without plasmonic section.

3. IN-PLANE CONFINEMENT. FURTHER REDUCTION OF THE PLASMONIC LOSS.

Additional contributor to plasmonic loss is the light scattering at the edge of the metal. Because of a substantial step between the refractive index of a metal and a dielectric, even a tiny roughness of the metal edge may cause a significant light scattering and, as a result, a substantial plasmonic loss³. The roughness of the metallic edge substantially depends on the metal fabrication technology. In general, the edge roughness is worse for the lift-off fabrication technique than for the Ar-milling-based technique. In each case, the substantial contribution to the plasmonic loss due the light scattering at the metal edge can be reduced by optimizing the in-plane confinement of a surface plasmon.

Often a metal stripe is used for the in-plane confinement of a plasmon (Fig.4 (a)). In this case, a surface plasmon propagates just under the metallic stripe. Even though the fabrication of a stripe-type plasmonic waveguide is very simple, the propagation loss of a surface plasmon in such a structure is very high. It is because there is a substantial amount of the plasmon optical field at the metal edge and the light scattering is large. When it is possible, the stripe confinement of Fig.4(a) should be avoided in order to obtain a low propagation loss of a plasmon.

We have studied 3 types of optimized in-plane confinement^{7,9,14} for a surface plasmon: wedge-type, bridge-type and groove type. All these types of the in-plane confinement are effective to reduce the propagation loss of a plasmon. The reason for the reduction is the removal of light from the vicinity of the metal edge and, therefore, the reduction of light scattering. Figure 4 shows the calculated distribution of the optical field of a surface plasmon in yellow color. Only in the case of the stripe-confinement, there is an optical field at the metal edge. In other cases, there is practically no optical field at the metal edge and, as result, there is no light scattering.

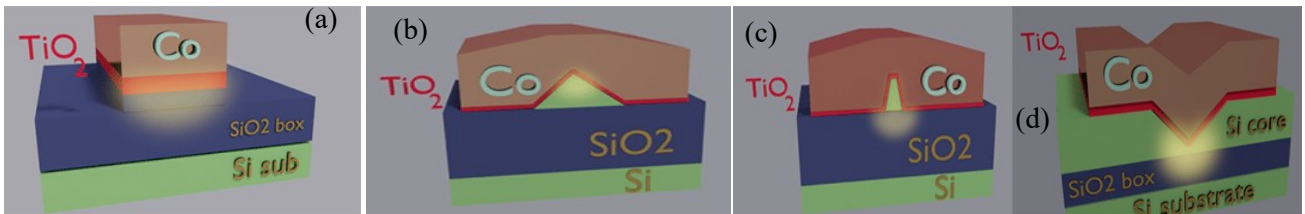


Figure 4 Lateral optical confinement of plasmons and measured plasmon propagation loss in $\text{Co}/\text{TiO}_2/\text{SiO}_2$ plasmonic structure. (a) metal stripe (8 $\text{dB}/\mu\text{m}$); (b) wedge-type (1.0 $\text{dB}/\mu\text{m}$); (c) bridge-type (0.7 $\text{dB}/\mu\text{m}$); (d) groove-type (1.2 $\text{dB}/\mu\text{m}$). The distribution of optical field is shown in yellow color. The propagation direction of a plasmon is perpendicularly to the page. Top and bottom Si is shown in green color.

All 3 types of the in-plane confinement are well compatible with the fabrication technology of a Si nanowire waveguide and a plasmonic waveguide. The optimized in-plane confinement was achieved by the following fabrication technology. In all 3 cases a Co/TiO₂ plasmonic waveguide is integrated with a Si nanowire waveguide. The top Si layer of SOI wafer is used for the in-plane confinement. In the case of a wedge-type plasmonic waveguide (Fig.4(b)), a Si stripe of width of 300 nm is left unetched in the plasmonic section. Next, this stripe is wet etched to make it wedge-shaped. In the case of the bridge-type plasmonic waveguide (Fig.4(c)), a Si stripe of width of 70 nm is left unetched in the plasmonic section. There is no following wet etching. For fabrication of a groove-type plasmonic waveguide (Fig.4(d)), a wide Si stripe of the width of 2 μm is left unetched in the plasmonic section. Next, a SiO₂ with a 200-nm-wide gap is fabricated on the top of it. The groove was wet etched through the gap in the SiO₂. Next, TiO₂ and metal are deposited after a removal of SiO₂. In all 3 fabrication cases, the metal strip is fabricated by the jet-lift-off technique. The width of the metal strip (~1.4 μm) was substantially wider than the width of the Si nanowire waveguide (~440 nm). The measured plasmon propagation loss was^{8,14,17} 1.2, 1.0 and 0.7 dB/μm, for groove-type, wedge-type and bridge-type of a Co/TiO₂/SiO₂ plasmonic structure (See Fig.4). In the case of a simplest stripe-type in-plane confinement (Fig.4(a)), the measured plasmon propagation loss was 8 dB/μm, which is unacceptably large. Since the fabrication technology of the bridge-type plasmonic waveguide is simplest and results in the smallest propagation loss of a surface plasmon, at present it is our choice for the fabrication technology for all our plasmonic structures.

4. IN-PARALLEL INTEGRATION OF THE PLASMONIC AND SI WAVEGUIDES

Even though the plasmon propagation loss can be reduced to a negligible value, the problem of a high coupling loss between plasmonic and Si waveguides remains the main obstacle for a wide application of the plasmonic devices. Even in the case when the propagation loss would be fully neglected, the coupling loss of 4 dB (See Fig.2) means that the minimum loss of a plasmonic device is 8 dB. This value is unacceptably large for many applications. We have tried unsuccessfully several methods to reduce the coupling loss. It is difficult to reduce the coupling loss below 3-4 dB/facet, because of a large difference of distribution of optical field of a surface plasmon and a waveguide mode, and because of the length limitation of a possible mode converter to about 1-2 μm.

One method to avoid the high coupling loss between the plasmonic and Si waveguide is the usage of an in-parallel integration scheme instead of the series integration. In the case of the in-parallel integration, light is coupled side-to-side between plasmonic and Si waveguides and there is no issue of the coupling loss between them. However, there is a problem with the in-parallel integration. If, in the case of the in-series integration, the light scattering at the metal edge can be avoided (see previous section), this scattering is unavoidable for the in-parallel integration. For this reason, we have not succeeded in a fabrication of an in-parallel integrated plasmonic waveguide using the jet-lift-off fabrication method, which has been successfully used for the in-series integration. It is because of the insufficient smoothness of the metal edge obtained by this technology. When we switched from the jet-lift-off method to the Ar-milling method for the fabrication of metal for the plasmonic section, a reasonably-low insertion loss was obtained.

The insertion for in-parallel integration depends on the gap width between the Si and plasmonic waveguides. In the case

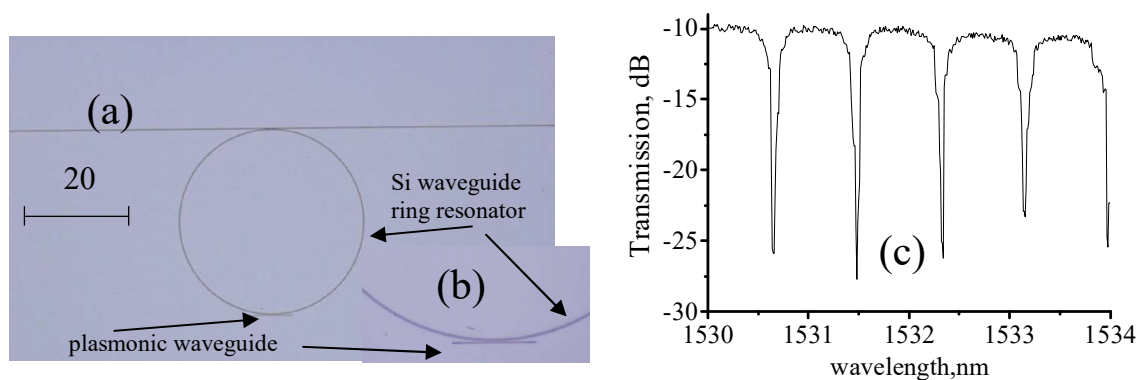


Figure 5. Plasmonic isolator of ring-resonator type. (a) Top view. The ring resonator is made of a Si nanowire waveguide. At the bottom there is a plasmonic waveguide, which is coupled to the ring. (b) Magnification of plasmonic part. (c) Transmission⁷ of the ring resonator, when the gap between the ring and plasmonic waveguide is 600 nm.

of the integration of a Si-nanowire waveguide and a Co/TiO₂/SiO₂ plasmonic waveguide, the total insertion loss of 0.9 dB and 2 dB at $\lambda=1550$ nm was measured for gap between waveguides of 600 nm and of 250 nm, respectively^{6,8,15}. The bridge-type of the in-plane conformer (Fig.4(c)) is still very effective for the loss reduction and always has been used in the case of the in-parallel integration.

5. PLASMONIC ISOLATOR

The optical isolator is transparent in one direction, and it blocks light in the opposite direction. It protects optical elements from unwanted back reflection. The integration of an optical isolator is important for PIC, because the problem of back-reflected light is more severe in the case of integrated optical elements^{2,18-25}. A new design of an integrated optical isolator, which utilizes unique non-reciprocal properties of a surface plasmon, has been proposed^{2,3}. The merits of the plasmonic isolator are a small size and a good compatibility of its fabrication technology with the fabrication technology of the PIC¹⁵.

Figure 3(a) shows a design of the plasmonic isolator integrated in-series with a Si waveguide. As was explained in Section 2, light can reach from the input fiber to output fiber only because a surface plasmon is excited at Co-TiO₂/SiO₂ interface. The Co is magneto-optical material, and its optical properties are non-reciprocal. It means that they are different for two opposite directions of light propagation. The plasmonic waveguide containing the Co is optimized^{7,17} so that a plasmon is excited in one direction, but a surface plasmon cannot be excited in the opposite direction. Therefore, light can pass from input to output only in the forward direction, but light is blocked in the opposite direction. The isolation of this design is proportional to the isolator length. As has been explained in Section 4, the yet-unsolved problem of this design is the coupling loss between plasmonic and Si waveguides, which can be resolved by using parallel integration. We have fabricated and studied a ring-type, a Mach-Zehnder type and non-reciprocal coupler type of the plasmonic isolator, which utilize the parallel integration.

Figure 5(a) shows the fabricated plasmonic isolator of the ring-resonator type^{15,17}. The ring resonator is made of a Si nanowire waveguide. At the bottom of the ring there is a plasmonic waveguide. Light is coupled between the ring and plasmonic waveguide. Figure 5(b) shows the measured transmission of the fabricated device. There are narrow peaks, which correspond to the resonance frequency of the ring resonator. Because of non-reciprocal optical properties of the plasmonic waveguide, the positions of the resonance peaks are slightly different for opposite directions of light propagation. When the wavelength of light is in the vicinity of a resonance peak, the transmission is different for opposite directions of light propagation and the device functions as an optical isolator.

Figure 6(a) shows the fabricated plasmonic isolator based on a Mach-Zehnder interferometer^{15,17}. The Mach-Zehnder interferometer is made of a Si nanowire waveguide. The input light is split into two arms of the interferometer by a 50% directional coupler. At output the light from both arms are combined by the second 50% directional coupler. When there is no phase difference between light passing each arm, the combined light is coupled into the first output port. When the

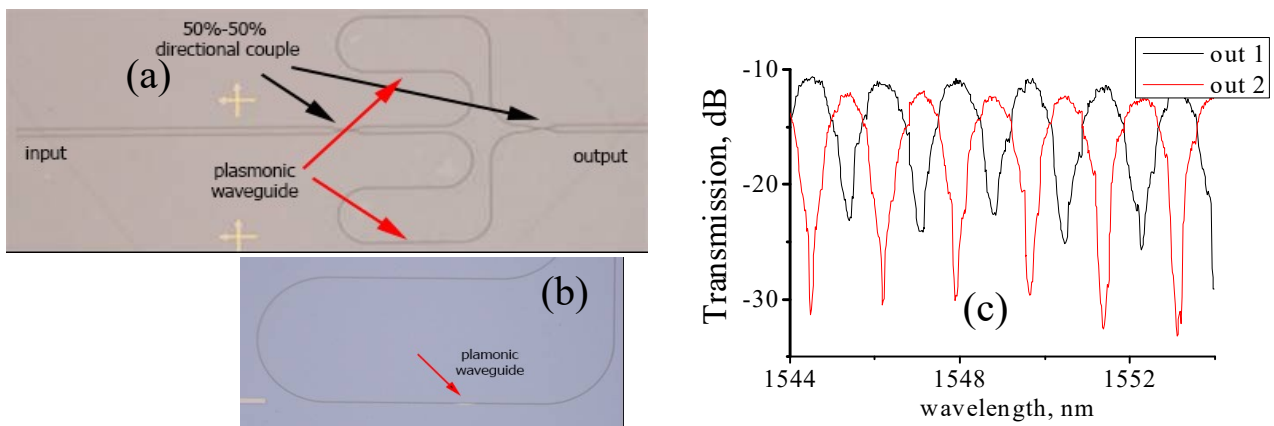


Figure 6. Plasmonic isolator based on a Mach-Zehnder interferometer. (a) Top view. (b) Magnification of plasmonic part. (c) Transmission⁷ of the asymmetric interferometer vs wavelength. The gap between the ring and plasmonic waveguide is 600 nm. Length difference of arms is 200 μm .

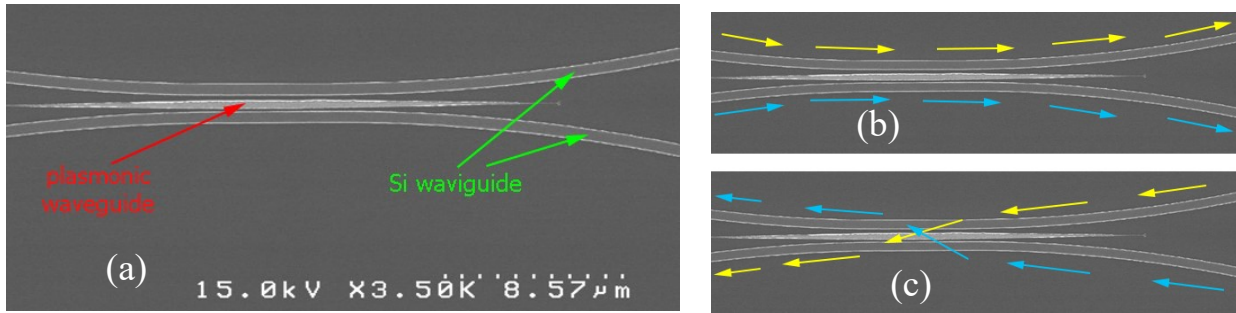


Figure 7 Top view of plasmonic isolator based on a non-reciprocal coupler. There is a plasmonic waveguide between two Si nanowire waveguides; (a) Light path in forward direction; (b) Light path in backward direction. Yellow arrows show light coupled into input 1. Blue arrows show light coupled into input 2

phase difference is 180 degrees, the light is coupled into the second output port.

There is a plasmonic waveguide in the vicinity of each arm of the interferometer (Fig.6b). The position of the plasmonic waveguide is different for the upper and lower arm. Even though two plasmonic waveguides are magnetized in the same direction, their magnetization directions are different in respect to the light propagation direction. For the upper arm, the magnetization is toward the right hand. For the lower arm, the magnetization is toward the left hand. Therefore, light experiences the opposite magneto-optical effect in two arms of the interferometer. As a result, the phase difference between light passing each arm is 0 degree in forward direction and 180 degrees in the backward direction. Therefore, in the forward direction the light passes from the input to the output. The unwanted reflected light in the backward direction is blocked from the input. Figure 6(c) shows the measured fiber-to-fiber transmission for the output 1 and output 2. Despite the plasmonic sections, the on/off ratio is still substantial (~15-20 dB).

Figure 7(a) shows the fabricated plasmonic isolator based on a non-reciprocal coupler¹⁷. It consists of two coupled Si nanowire waveguides and a plasmonic waveguides between them. The width of the Si nanowire waveguide is 450 nm. The width of the plasmonic waveguide is 300 nm. The gap is 100 nm at both sides of the plasmonic waveguide. Light is coupled from one Si nanowire waveguide into a plasmonic waveguide. Next, depending on the coupling parameters light either is coupled back into the same Si nanowire waveguide or it is coupled into another Si nanowire waveguide. Because of the non-reciprocal properties of the plasmonic waveguide, the coupling between two Si nanowire waveguides is different for two opposite light propagation directions. The coupler can be adjusted so that in the forward direction the light passes through the same Si waveguide (Fig. 7(b)), but in the backward direction the light is fully coupled from one Si waveguide to another. Therefore, the coupler operates as an optical isolator.

As was explained in Section 4, the light scattering at the metal edge mostly contributes to the insertion loss in the case of the parallel integration. In the case of the non-reciprocal coupler, the scattering should be optimized at two edges simultaneously. It is a difficult task. Till present we have not succeeded to reduce the insertion loss of the non-reciprocal coupler below ~ 15-20 dB. An improvement of the metal edge smoothness by further optimizing the Ar- milling technique might be a solution.

6. CONCLUSION

The fabrication technology of a plasmonic waveguide with a low propagation loss has been described for both the “plasmon- friendly” and the “plasmon- unfriendly” metals. Using this fabrication technology, different metals of different unique properties could be used in the plasmonic structures, additionally to traditionally-used gold. Feasibility of a dense integration of optical components made of plasmonic and Si waveguides is a major merit of the developed technology.

The ability to enhance the magneto-optical effect is a unique and important property of a surface plasmon. As a result, plasmonic structures, which contain a ferromagnetic metal, have unique non-reciprocal properties, which have been utilized in order to fabricate a plasmonic isolator. The plasmonic isolator benefits from a dense optical integration, because of its small size and its good compatibility with present fabrication technology of the Photonic Integrated Circuits.

We have fabricated a Co-based plasmonic waveguide with a low propagation loss of 0.7 dB/ μm . at $\lambda=1550$ nm. We have monolithically integrated this plasmonic waveguide with a Si nanowire waveguide with a moderate coupling loss of 4 dB per a facet in the case of a serial integration. In the case of the parallel integration, the low insertion loss of 0.9 dB and 2 dB at $\lambda=1550$ nm was demonstrated for the gap between a Co-based plasmonic waveguide and a Si waveguide of 600 nm and of 250 nm, respectively. Utilizing this technology, we have fabricated, optimized and studied the plasmonic isolators of the ring-type, the Mach–Zehnder type and the non-reciprocal coupler type.

REFERENCES

- [1] Armelles, G., Cebollada, A., García-Martín, A. and González, M. U., “Magnetoplasmonics: Combining Magnetic and Plasmonic Functionalities,” *Adv. Opt. Mater.* **1**(1), 10–35 (2013).
- [2] Zayets, V., Saito, H., Yuasa, S. and Ando, K., “Enhancement of the transverse non-reciprocal magneto-optical effect,” *J. Appl. Phys.* **111**(2), 023103 (2012).
- [3] Zayets, V., Saito, H., Ando, K. and Yuasa, S., “Optical Isolator Utilizing Surface Plasmons,” *Mater.* 2012, Vol. 5, Pages 857-871 **5**(5), 857–871 (2012).
- [4] Sinatkas, G., Christopoulos, T., Tsilipakos, O. and Kriezis, E. E., “Electro-optic modulation in integrated photonics,” *J. Appl. Phys.* **130**(1), 010901 (2021).
- [5] Kaihara, T., Shimizu, H., Dicken, M. J., Sweatlock, L. A., Pacifici, D., Lezec, H. J., Bhattacharya, K. and Atwater, H. A., “Nonreciprocal dielectric-loaded plasmonic waveguides using magneto-optical effect of Fe,” *Opt. Express*, Vol. 25, Issue 2, pp. 730-748 **25**(2), 730–748 (2017).
- [6] Zayets, V., Saitoh, H. and Yuasa, S., “Technologies to reduce insertion loss of plasmonic isolator integrated with Si nanowire waveguides,” *Conf. Solid State Devices Mater. (SSDM)*, PS 5-06, Tokyo (2018).
- [7] Shimizu, H. and Zayets, V., “Plasmonic isolator for photonic integrated circuits,” *MRS Bull.* **43**(06), 425–429 (2018).
- [8] Zayets, V., Saito, H. and Yuasa, S., “Fabrication technology of low-propagation-loss plasmonic waveguide containing a ferromagnetic metal.,” *Intermag*, AI-05, Singapore (2018).
- [9] Merzlikin, A. M. and Baryshev, A. V., “Tunable plasmonic thin magneto-optical wave plate,” *JOSA B*, Vol. 33, Issue 7, pp. 1399-1405 **33**(7), 1399–1405 (2016).
- [10] Kaihara, T., Shimizu, H., Cebollada, A. and Armelles, G., “Magnetic field control and wavelength tunability of SPP excitations using Al₂O₃/SiO₂/Fe structures,” *Appl. Phys. Lett.* **109**(11), 111102 (2016).
- [11] Johnson, P. B. and Christy, R. W., “Optical constants of transition metals: Ti, V, Cr, Mn, Fe, Co, Ni, and Pd,” *Phys. Rev. B* **9**(12), 5056 (1974).
- [12] Zayets, V., Saito, H., Ando, K. and Yuasa, S., “Long-distance propagation of a surface plasmon on the surface of a ferromagnetic metal,” *Opt. Express* **23**(10) (2015).
- [13] Kaihara, T., Ando, T., Shimizu, H., Zayets, V., Saito, H., Ando, K. and Yuasa, S., “Enhancement of magneto-optical Kerr effect by surface plasmons in trilayer structure consisting of double-layer dielectrics and ferromagnetic metal,” *Opt. Express* **23**(9) (2015).
- [14] Zayets, V., Saito, H. and Yuasa, S., “Photonic integration of plasmonic Magneto-optical waveguide and Si nanowire waveguide,” *Proc. 2017 IEEE 7th Int. Conf. Nanomater. Appl.*

- Prop. N. 2017 **2017-Janua** (2017).
- [15] Shimizu, H. and Zayets, V., “Plasmonic isolator for photonic integrated circuits,” *MRS Bull.* **43**(6), 425–429 (2018).
 - [16] Zayets, V., Saito, H. and Yuasa, S., “Photonic integration of plasmonic Magneto-optical waveguide and Si nanowire waveguide,” *Proc. 2017 IEEE 7th Int. Conf. Nanomater. Appl.* Prop. N. 2017 **2017-January** (2017).
 - [17] Zayets, V., Saito, H. and Yuasa, S., “Photonic integration of plasmonic Magneto-optical waveguide and Si nanowire waveguide,” *2017 IEEE 7th Int. Conf. Nanomater. Appl. Prop.*, 04NESP17-1-04NESP17-6, IEEE (2017).
 - [18] Stadler, B. J. H. and Mizumoto, T., “Integrated magneto-optical materials and isolators: A review,” *IEEE Photonics J.* **6**(1) (2014).
 - [19] Shoji, Y. and Mizumoto, T., “Silicon Waveguide Optical Isolator with Directly Bonded Magneto-Optical Garnet,” *Appl. Sci.* 2019, Vol. 9, Page 609 **9**(3), 609 (2019).
 - [20] Saito, H., Ando, K., Yuasa, S. and Zayets, V., “Magnetization-dependent loss in an (Al,Ga)As optical waveguide with an embedded Fe micromagnet,” *Opt. Lett.* Vol. 35, Issue 7, pp. 931-933 **35**(7), 931–933 (2010).
 - [21] Shimizu, H. and Nakano, Y., “First demonstration of TE mode nonreciprocal propagation in an InGaAsP/InP active waveguide for an integratable optical isolator,” *Japanese J. Appl. Physics, Part 2 Lett.* **43**(12 A), L1561 (2004).
 - [22] Shimizu, H. and Nakano, Y., “Monolithic integration of a waveguide optical isolator with a distributed feedback laser diode in the 1.5- μm wavelength range,” *IEEE Photonics Technol. Lett.* **19**(24), 1973–1975 (2007).
 - [23] Shimizu, H. and Nakano, Y., “Fabrication and characterization of an InGaAsP/InP active waveguide optical isolator with 14.7 dB/mm TE mode nonreciprocal attenuation,” *J. Light. Technol.* **24**(1), 38–43 (2006).
 - [24] Zaets, W. and Ando, K., “Optical waveguide isolator based on nonreciprocal loss/gain of amplifier covered by ferromagnetic layer,” *IEEE Photonics Technol. Lett.* **11**(8), 1012–1014 (1999).
 - [25] Van Parys, W., Moeyersoon, B., Van Thourhout, D., Baets, R., Vanwollegem, M., Dagens, B., Decobert, J., Le Gouezigou, O., Make, D., Vanheertum, R. and Lagae, L., “Transverse magnetic mode nonreciprocal propagation in an amplifying AlGaInAs/InP optical waveguide isolator,” *Appl. Phys. Lett.* **88**(7), 071115 (2006).